Available online at www.sciencedirect.com
SCIENCE DIRECT®
Journal of Computational Physics 211 (2006) 129–153
JOURNAL OF COMPUTATIONAL PHYSICS
www.elsevier.com/locate/jcp

Convergence properties of Monte Carlo functional expansion tallies

David P. Griesheimer *, William R. Martin, James Paul Holloway

Department of Nuclear Engineering and Radiological Sciences, University of Michigan, 2355 Bonisteel Boulevard, 1906 Cooley Bldg., Ann Arbor, MI 48109, United States

Received 24 June 2004; received in revised form 5 May 2005; accepted 18 May 2005
Available online 20 July 2005

Abstract

The functional expansion tally (FET) is a method for constructing functional estimates of unknown tally distributions via Monte Carlo simulation. This technique uses a Monte Carlo calculation to estimate expansion coefficients of the tally distribution with respect to a set of orthogonal basis functions. The rate at which the FET approximation converges to the true distribution as the expansion order is increased is developed. For sufficiently smooth distributions the FET is shown to converge faster, and achieve a lower residual error, than a histogram approximation.

Keywords: Monte Carlo; Functional expansion; Surface crossing estimator; Tally; Legendre polynomials

1. Introduction

Monte Carlo simulations are fundamentally nothing more than a stochastic numerical experiment. In order to solve a particular problem with the Monte Carlo method, a user must set up a simulation of the physical system under consideration. If the simulation accurately recreates the behavior of the system, then the results of the simulation will be an estimate of the expected outcome of the system. Monte Carlo methods are widely used in particle transport and radiation transport calculations [1–4] to study transport processes within complex systems. In these applications, particles are sampled from a source distribution defined over the problem geometry. A random walk for each particle is then simulated, based on the physical properties of the system. Each particle is tracked until termination, typically through absorption or leakage from the system.

* Corresponding author. Tel.: +1 734 678 1038; fax: +1 734 763 4540.
E-mail address: dgrieshe@umich.edu (D.P. Griesheimer).

0021-9991/$ - see front matter
doi:10.1016/j.jcp.2005.05.023

Typically, Monte Carlo particle transport simulations are performed to estimate a reaction rate in a given volume or leakage rate across a given surface. Over the past 50 years a variety of statistical estimators (tallies) for these quantities have been developed [1,3–7]. For example, by simply counting the number of particles that pass through a region, an accurate estimate of the integrated flux (i.e. scalar flux) can be obtained. Moreover, slight variations in this estimator lead to many other tallies, such as absorption tallies, fission source tallies, and fission heating tallies. All of these variations are based on the product of a known function (cross section, fission Q-function, etc.) against the particle flux or current distribution within a region. Due to the nature of the Monte Carlo method, these tallies have traditionally been limited for use in estimating integral (i.e. region-averaged) quantities. There are, however, many situations where a higher level of detail is desired. Instead of simply estimating the integral of the distribution, it is often useful to also obtain an estimate for the shape of the distribution. Such situations are especially common in particle transport calculations where the spatial and/or angular distributions of particle flux are often quantities of interest.

In order to obtain higher order shape information from Monte Carlo simulations, such as the phase space (energy, space, time, angle, etc.) dependence of a particle flux distribution, the traditional approach has been to simply divide the phase space into bins and calculate an average over each bin, resulting in a histogram approximation to the true tally distribution. If many bins are used in the histogram, such an approach can lead to large statistical uncertainties in the resulting approximation because each phase space bin is sampled relatively few times.

An alternative approach is to use Monte Carlo to estimate functional expansion coefficients of the true distribution with respect to some set of (usually orthogonal) basis functions. The set of expansion coefficients can then be used to construct a continuous functional approximation of the true distribution. This technique, referred to as the ''functional expansion technique'' or ''functional expansion tally'' (FET) offers several benefits over conventional histogram-style Monte Carlo tallies. The main advantage is that every score in the region contributes to every expansion coefficient, yielding information regarding the shape of the phase space distribution as well as its average value. Moreover, it is possible to choose the basis functions such that the lowest order term preserves the integral quantity over the region of interest, hence preserving the average value estimated by the conventional tallies. Therefore, the FET extracts higher order information from the random walk than is possible with traditional Monte Carlo tallies.

The FET was first proposed by Chadsey et al. [8] who demonstrated that a Monte Carlo simulation can be used to estimate the spherical harmonic expansion coefficients of the angular distribution of X-ray photoemission. Their results show that the use of a functional expansion representation of the angular distribution has several advantages over a traditional discrete histogram approximation. One advantage is that the estimated solution is a continuous function, which can be more convenient for subsequent analysis. But more importantly the authors also claim, although no numerical results or formal proof was presented, that the FET can offer ''substantial variance reduction'' if an appropriate set of basis functions is used.

A follow up paper by Beers and Pine [9] generalized the FET for any Monte Carlo simulation. A detailed mathematical formulation of the method was given for both expansions of the probability density of a random variable and functions defined on a stochastic process. The applicability of these methods was demonstrated for electron transport problems using Legendre polynomials and spherical harmonics as basis sets. Subsequent studies have applied the FET to a variety of applications [10–20] but there has been a lack of work regarding the convergence properties of the FET.

In this paper, we present a mathematical analysis of the convergence properties of the FET for Monte Carlo calculations. This paper demonstrates that the FET can often provide a better approximation for the shape of an unknown tally distribution than a traditional histogram tally. To achieve this result, we consider the application of the FET and histogram approximations to the set of all continuous distributions

defined over an expansion domain. To quantify the accuracy of each approximation we use the 2-norm measure of the residual error between the estimated tally and the true tally. For both the FET and histogram tallies we show that the accuracy of the final approximation depends on two sources of error: truncation and statistical.

Truncation error in the FET arises from approximating a function with a finite series expansion. The magnitude of the truncation error is not affected by the number of histories used in the Monte Carlo simulation but, instead, depends only on the expansion order of the approximation. It should be noted that truncation error also affects the histogram tally, due to approximating a continuous function with a series of flat line segments.

Statistical error in both the FET and histogram tallies is due to the stochastic nature of the Monte Carlo simulation. When functional expansion coefficients, tallied by Monte Carlo, are used to reconstruct a functional approximation, the uncertainties in each "mode" combine and can cause significant contamination of the final result.

To estimate expansion coefficients, the FET relies on the Monte Carlo random walk to perform a numerical integration over the individual basis functions. For higher order expansion coefficients the corresponding basis functions oscillate rapidly over the phase space and may be difficult to integrate numerically. As a result, the statistical uncertainty of individual expansion coefficients increases with the order of the coefficient.

Histogram tallies use Monte Carlo to numerically evaluate the integral of the distribution over small bins that partition the tally domain. As the number of histogram bins increases, the width of each bin decreases, resulting in fewer scores, and a larger variance, in each bin.

Both the FET and histogram tallies involve a tradeoff between sources of statistical and truncation errors. Increasing the approximation order (or the number of histogram bins) will decrease the truncation error but increase the statistical uncertainty of the approximation. Decreasing the approximation order will have the opposite effect. In this paper we show that, for a fixed number of histories run, an optimal approximation order exists, which minimizes the residual error of the approximation in the 2-norm. Furthermore, we also show that the 2-norm error of the FET approximation is less than the corresponding error of the histogram approximation, for large classes of general distribution shapes.

2. Foundation and derivation of the FET

Before beginning the actual derivation of the FET it is useful to consider an instructive example from particle transport. Suppose we wish to estimate an integral of the form

$$\int f(\vec{r})\phi(\vec{r})\mathrm{d}^3 r, \tag{1}$$

where $\phi(\vec{r})$ is the scalar flux distribution over some volume V. If we use a Monte Carlo process to count (i.e. sample) the number of particle interactions that occur within this volume, then it is useful to rewrite Eq. (1) as

$$\int f(\vec{r})\phi(\vec{r})\mathrm{d}^3 r = \int \frac{f(\vec{r})}{\Sigma(\vec{r})}\Sigma(\vec{r})\phi(\vec{r})\mathrm{d}^3 r, \tag{2}$$

where $\Sigma(\vec{r})$ is the total cross section in V. The factor $\Sigma(\vec{r})\phi(\vec{r})$ inside the integral in Eq. (2) gives the reaction rate of particles within the volume. This reaction rate can be converted into a probability distribution function by normalizing by the total number of reactions within V

$$P(\vec{r}) = \frac{\Sigma(\vec{r})\phi(\vec{r})}{\int f(\vec{r})\phi(\vec{r})\mathrm{d}^3 r}. \tag{3}$$

Eq. (3) expresses the probability $P(\vec{r})\mathrm{d}^3r$ that a particle interaction within the volume V will occur in d^3r about position $\vec{r}$. This result can be used to rewrite Eq. (2) as

$$\int f(\vec{r})\phi(\vec{r})\mathrm{d}^3r = \int \tilde{f}(\vec{r})P(\vec{r})\mathrm{d}^3r, \tag{4}$$

where

$$\tilde{f}(\vec{r}) = \frac{f(\vec{r})}{\Sigma(\vec{r})}\left(\int f(\vec{r})\phi(\vec{r})\mathrm{d}^3r\right). \tag{5}$$

From Eq. (4) we see that all of the information about the shape of the flux is captured in $P(\vec{r})$, the probability density function (pdf) for particle interaction locations in the volume. While we still have no a priori information about the shape of $P(\vec{r})$, it is easily sampled during a Monte Carlo simulation. In fact, every particle interaction that occurs in V during the simulation provides a valid sample from $P(\vec{r})$.

Given this example, it is important to stress that the results presented in this paper are not limited to particle or radiation transport applications. Indeed, an approach similar to that presented above can be used to show that a pdf $P(x)$ can be defined to capture the functional dependence of any quantity $T(x)$ that we wish to investigate. For subsequent analysis, we assume that the distribution of $T(x)$ is not known a priori and that we wish to estimate its higher order properties from a set of independent realizations of $T(x)$ obtained during a Monte Carlo simulation. For the remainder of this paper, we will work with the associated pdf $P(x)$, rather than $T(x)$, for convenience in our error and convergence analysis.

It is important to recognize that the distribution $P(x)$ is never directly sampled (or resampled) by conventional sampling methods during the Monte Carlo process. Rather, this pdf describes the probability that certain types of random events will occur at specific phase locations during the Monte Carlo simulation. Thus the Monte Carlo algorithm naturally produces samples from $P(x)$ (i.e. the positions of events that actually occur) as the simulation progresses. In essence, a Monte Carlo simulation can be viewed as a complex sampling algorithm for obtaining realizations from some physically meaningful distribution $P(x)$. It is the goal of the FET to reconstruct information about $P(x)$ from the individual samples produced during the simulation.

It is worth noting that the reconstruction of an unknown pdf from individual samples has long been a broad area of research in the field of statistics. A large body of research on techniques such as kernel density estimation (KDE) is widely available in the literature [21,22]. Many of these statistical techniques employ a nonparametric approach to obtain a best fit without guidance (or constraints) from the underlying physics that govern the process. While there is some overlap between the KDE method and the FET, we specifically wish to narrow our focus to consider those results that are most applicable to Monte Carlo tallies. In many cases, developing a specific functional expansion tally (e.g. defining a tally domain and choosing a tailored set of basis functions) in order to preserve some physical properties of the actual distribution will result in a more accurate and robust solution than is possible with other statistical reconstruction techniques.

2.1. Derivation of the FET estimators

We begin the derivation of the FET by considering an accurate Monte Carlo algorithm that produces independent realizations of a random variable x from a probability density function $P(x)$. The traditional approach for obtaining shape information for $P(x)$ is to divide the domain of the random variable into "bins", $b = \{1,2, \ldots, M\}$, and then count the number of events that occur in each bin, N_b, during the simulation. The total score in a bin, N_b , divided by the number of independent trials, N, is an unbiased estimator for the probability that a given realization will fall within the bin,

$$E\left[\frac{N_b}{N}\right] = P(x_{b-1} \leqslant x < x_b), \tag{6}$$

where x_{b-1} and x_b denote the bounds of bin b. When this process is repeated for all of the bins, the result is a histogram approximation to the actual pdf,

$$P(x) = \sum_{b=1}^{M} \left(\overline{P_{M,b}^{\text{hist}}}(x) + \mathrm{O}[\Delta x_b]\right), \tag{7}$$

where

$$\overline{P_{M,b}^{\text{hist}}}(x) = \frac{P(x_{b-1} \leqslant x < x_b)}{\Delta x_b}, \tag{8}$$

Δx_b is the width of bin b, and $\overline{P_{M,b}^{\text{hist}}}(x)$ is the true value of the histogram in bin b. As the number of bins, M, is increased, the truncation error decreases and the histogram approximation converges to the continuous distribution.

In the FET the unknown pdf $P(x)$ is represented as a series expansion in a complete set of basis functions. The set of independent samples from $P(x)$ are then used to estimate the coefficients of the expansion. To show this, let $\{\psi_n\}_0^\infty$ be a complete orthogonal set with respect to a weighting function ρ in $L_\rho^2(\Gamma)$, the space of all square integrable functions over some bounded domain Γ. It then follows that any $P(x) \in L_\rho^2(\Gamma)$ can be written as

$$P(x) = \sum_{n=0}^{\infty} \bar{a}_n k_n \psi_n(x), \tag{9}$$

where $\bar{a}_n$ is the true nth expansion coefficient defined by the inner-product,

$$\bar{a}_n = \int_\Gamma \psi_n(x)\rho(x)P(x)\mathrm{d}x, \tag{10}$$

and k_n is the normalization constant for the nth basis function [23],

$$k_n = \frac{1}{\|\psi_n\|^2}. \tag{11}$$

In order to create a functional approximation to $P(x)$ using Eq. (9), the expansion coefficients $\bar{a}_n$ must first be determined. The coefficients are calculated using Eq. (10), a convenient integral that is ideal for estimation by Monte Carlo methods. In fact, it is easily shown that the sample statistic

$$\hat{a}_n = \frac{1}{N}\sum_{i=1}^{N} \psi_n(x_i)\rho(x_i) \tag{12}$$

is an unbiased analog estimator for the true expansion coefficient $\bar{a}_n$ [9,10].

3. Variance of the FET estimator

3.1. Variance of individual coefficients

It was established in the previous section (Eq. (10)) that the true expansion coefficient $\bar{a}_n$ is actually the expected value of the function $a_n = \psi_n(x)\rho(x)$,

$$\bar{a}_n = E[\psi_n(x)\rho(x)] = \int_\Gamma \psi_n(x)\rho(x)P(x)\mathrm{d}x. \tag{13}$$

From Eq. (13) it is straightforward to calculate the variance of $a_n(x)$,

$$\sigma^2_{a_n} = E\left[(\psi_n(x)\rho(x))^2\right] - E[\psi_n(x)\rho(x)]^2 = \int_\Gamma (\psi_n(x)\rho(x))^2 P(x)\mathrm{d}x - \bar{a}_n^2. \tag{14}$$

The true variance for an estimate of $\bar{a}_n$ made with N independent trials can now be written in terms of the true variance given in Eq. (14):

$$\sigma^2_{\bar{a}_n} = \frac{1}{N}\sigma^2_{a_n}. \tag{15}$$

Eqs. (14) and (15) give an analytic form for the true variance of expansion coefficients estimated by a Monte Carlo calculation. The sample variance of Eq. (15) provides an unbiased estimator of $\sigma^2_{\bar{a}_n}$ and can be calculated in the usual way,

$$\hat{\sigma}^2_{\bar{a}_n} = \frac{\sum_{i=1}^N (\psi_n(x_i)\rho(x_i))^2 - \frac{1}{N}\left(\sum_{i=1}^N \psi_n(x_i)\rho(x_i)\right)^2}{N(N-1)}. \tag{16}$$

Eq. (16) gives a measurement of the statistical uncertainty in each individual expansion coefficient.

3.2. Variance of the functional expansion

It is also possible to derive a more powerful and useful result that gives the pointwise variance of the reconstructed functional estimate rather than the individual coefficients. The derivation begins by considering a functional expansion of the distribution in some orthogonal basis set of functions,

$$P(x) = \sum_{n=0}^{M} a_n k_n \psi_n(x). \tag{17}$$

As shown in Eq. (7), any set of N independently observed events can be used to estimate any or all members of the set of expansion coefficients $\{\bar{a}_n\}_0^\infty$. Therefore, a single history i provides an estimate $\hat{\alpha}_{n,i}$,

$$\hat{\alpha}_{n,i} = \psi_n(x_i)\rho(x_i) \tag{18}$$

for every expansion coefficient in the set $\{\bar{\alpha}_{n,i}\}_0^M$. This set of expansion coefficients can, in turn, be used in Eq. (17) to produce a single history estimate for the function $P(x)$ itself. At this point, it is useful to define a new quantity, $\widehat{P_{M,i}}(x)$, that represents an Mth order estimate of the function $P(x)$ resulting from only the ith observed event,

$$\widehat{P_{M,i}}(x) = \sum_{n=0}^{M} \hat{\alpha}_{n,i} k_n \psi_n(x). \tag{19}$$

Taking the average of the $\widehat{P_{M,i}}(x)$ over N observations yields an intermediate result,

$$\widehat{P_M}(x) = \frac{1}{N}\sum_{i=1}^{N} \widehat{P_{M,i}}(x) = \frac{1}{N}\sum_{i=1}^{N}\sum_{n=0}^{M} \hat{\alpha}_{n,i} k_n \psi_n(x), \tag{20}$$

which can be simplified to yield

$$\widehat{P_M}(x) = \sum_{n=0}^{M} k_n \psi_n(x)\left(\frac{1}{N}\sum_{i=1}^{N}\hat{\alpha}_{n,i}\right) = \sum_{n=0}^{M} \hat{a}_n k_n \psi_n(x). \tag{21}$$

Eq. (21) gives the expected result, in which the mean functional expansion $\widehat{P_M}(x)$ for N independent trials is equal to the functional expansion that uses the sample mean for each expansion coefficient individually.

A more interesting result occurs when the sample variance formula is applied to N independent realizations of $\widehat{P_{M,i}}(x)$,

$$\hat{\sigma}^2_{\widehat{P_M}}(x) = \frac{\sum_{i=1}^{N}\left(\widehat{P_{M,i}}(x)\right)^2 - N\left(\widehat{P_M}(x)\right)^2}{N(N-1)}. \tag{22}$$

Eq. (22) can be algebraically manipulated to give the final result,

$$\begin{aligned}
\hat{\sigma}^2_{\widehat{P_M}}(x) &= \frac{\sum_{i=1}^{N}\left(\sum_{n=0}^{M}\hat{\alpha}_{n,i}k_n\psi_n(x)\right)^2 - N\left(\sum_{n=0}^{M}\hat{a}_n k_n\psi_n(x)\right)^2}{N(N-1)} \\
&= \frac{\sum_{i=1}^{N}\left(\sum_{n=0}^{M}\sum_{m=0}^{M}(\hat{\alpha}_{n,i}k_n\psi_n(x))(\hat{\alpha}_{m,i}k_m\psi_m(x))\right) - N\left(\sum_{n=0}^{M}\sum_{m=0}^{M}(\hat{a}_n k_n\psi_n(x))(\hat{a}_m k_m\psi_m(x))\right)}{N(N-1)} \\
&= \frac{1}{N-1}\sum_{n=0}^{M}\sum_{m=0}^{M}(k_n\psi_n(x))(k_m\psi_m(x))\frac{1}{N}\sum_{i=1}^{N}(\hat{\alpha}_{n,i}\hat{\alpha}_{m,i}) - \frac{1}{N-1}\left(\sum_{n=0}^{M}\sum_{m=0}^{M}(\hat{a}_n\hat{a}_m)(k_n\psi_n(x))(k_m\psi_m(x))\right) \\
&= \frac{1}{N-1}\sum_{n=0}^{M}\sum_{m=0}^{M}(k_n\psi_n(x))(k_m\psi_m(x))\widehat{\alpha_{n,i}\alpha_{m,i}} - \frac{1}{N-1}\left(\sum_{n=0}^{M}\sum_{m=0}^{M}(\hat{a}_n\hat{a}_m)(k_n\psi_n(x))(k_m\psi_m(x))\right) \\
&= \frac{1}{N-1}\sum_{n=0}^{M}\sum_{m=0}^{M}(\widehat{\alpha_{n,i}\alpha_{m,i}} - \hat{a}_n\hat{a}_m)(k_n\psi_n(x))(k_m\psi_m(x)) \\
\hat{\sigma}^2_{\widehat{P_M}}(x) &= \frac{N}{N-1}\sum_{n=0}^{M}\sum_{m=0}^{M}\hat{\sigma}_{a_n a_m}(k_n\psi_n(x))(k_m\psi_m(x)),
\end{aligned} \tag{23}$$

where $\hat{\sigma}_{a_n a_m}$ is, by definition, the sample covariance between estimates of $\hat{a}_n$ and $\hat{a}_m$.

Eq. (23) gives the variance (as a function of x) for the estimated functional expansion of the distribution. Unfortunately, this equation for the variance requires the covariance between every combination of expansion coefficients to be calculated. Computing the covariance matrix for a large number of expansion coefficients can increase the memory requirements and run time of a Monte Carlo simulation. To prevent this burden on the code, it is useful to consider an estimate for the 2-norm of this functional variance.

3.3. Two-norm variance of the functional expansion

The derivation of the 2-norm variance estimate begins with the sample variance for $\widehat{P_M}(x)$, given in Eq. (22). By expanding, integrating both sides over Γ, and using the orthogonal properties of the basis set $\{\psi_n\}_0^M$, Eq. (22) can be manipulated to give,

$$\begin{aligned}
&\int_\Gamma \hat{\sigma}^2_{\widehat{P_M}}(x)\rho(x)\mathrm{d}x \\
&= \frac{\int_\Gamma \sum_{i=1}^{N}\left(\sum_{n=0}^{M}\sum_{m=0}^{M}(\hat{\alpha}_{n,i}k_n\psi_n(x))(\hat{\alpha}_{m,i}k_m\psi_m(x))\right)\rho(x) - \int_\Gamma N\left(\sum_{n=0}^{M}\sum_{m=0}^{M}(\hat{a}_n k_n\psi_n(x))(\hat{a}_m k_m\psi_m(x))\right)\rho(x)}{N(N-1)} \\
&= \frac{\sum_{i=1}^{N}\left(\sum_{n=0}^{M}\hat{\alpha}_{n,i}^2 k_n\right) - N\left(\sum_{n=0}^{M}\hat{a}_n^2 k_n\right)}{N(N-1)} = \frac{1}{(N-1)}\sum_{n=0}^{M}\left(\frac{1}{N}\sum_{i=1}^{N}\hat{\alpha}_{n,i}^2 k_n\right) - \frac{1}{N-1}\left(\sum_{n=0}^{M}\hat{a}_n^2 k_n\right) \\
&= \frac{1}{(N-1)}\sum_{n=0}^{M}\left(\widehat{\alpha_{n,i}^2} - \hat{a}_n^2\right)k_n,
\end{aligned}$$

which, in turn, can be simplified to yield

$$\int_\Gamma \underset{P_M}{\hat{\sigma}^2}(x)\rho(x)\mathrm{d}x = \sum_{n=0}^{M} \hat{\sigma}^2_{\bar{a}_n} k_n. \tag{24}$$

Eq. (24) gives an estimate of the statistical uncertainty in the entire functional expansion based only on the uncertainties in each of the individual expansion coefficients. Integrating Eq. (22), in effect, causes the covariance term to drop out of the equation, greatly simplifying the sample variance formula.

4. Theoretical convergence properties of the FET

Having established that Monte Carlo can be used to calculate a functional approximation to an unknown probability distribution, we now examine the accuracy of such an approach.

4.1. Truncation error

The functional expansion for $P(x)$ given in Eq. (9) is exact only if all terms in the series are included. Clearly it is not possible to estimate an infinite number of expansion coefficients and the functional approximation must be truncated at some finite number of terms M,

$$P(x) \approx P_M(x) = \sum_{n=0}^{M} \bar{a}_n k_n \psi_n(x). \tag{25}$$

This truncation after M terms introduces an error $E_M(x)$ in the estimation of $P(x)$ that is equal to the contributions from all expansion terms with $n > M$,

$$E_M(x) = (P(x) - P_M(x)) = \sum_{n=M+1}^{\infty} \bar{a}_n k_n \psi_n(x). \tag{26}$$

By Parseval's theorem [23], the rate at which the truncation error decreases is directly related to the rate at which the coefficients $|\bar{a}_n|$ go to zero. For non-analytic functions the expansion coefficients demonstrate algebraic convergence at a rate determined by κ, the algebraic index of convergence for the function $P(x)$ [24],

$$|\bar{a}_n| = \mathrm{O}\left[\frac{1}{n^\kappa}\right]. \tag{27}$$

The algebraic index of convergence is a constant value that depends on the smoothness of the function. For many common basis sets (e.g. Fourier, Chebyshev, and Legendre) the value of κ for a function is equal to the number of derivatives of the function that are square integrable. For analytic functions, the index of convergence is infinite and the expansion coefficients can converge exponentially fast. Further information on the convergence behavior for expansion coefficients in functional series approximations is widely available in many textbooks [23–25].

4.2. Statistical error

Another source of error in the FET arises from statistical uncertainty in the expansion coefficients. It is convenient to use the 2-norm to measure the total error between a stochastic FET approximation and the true function $P(x)$,

$$\|\hat{E}_M\| = \|P(x) - \hat{P}_{M,N}(x)\| = \sqrt{\int_\Gamma \left(P(x) - \hat{P}_{M,N}(x)\right)^2 \rho(x)\mathrm{d}x}, \tag{28}$$

where $\hat{P}_{M,N}(x)$ is the Monte Carlo estimate of the Mth order functional expansion approximation to $P(x)$ calculated using N independent particle histories. Eq. (28) can be rewritten as

$$\begin{aligned}\|\hat{E}_M\|^2 &= \int_\Gamma \left(\sum_{n=0}^{\infty} k_n \bar{a}_n \psi_n(x) - \sum_{n=0}^{M} k_n \hat{a}_n \psi_n(x)\right)^2 \rho(x)\mathrm{d}x \\ &= \int_\Gamma \left(\sum_{n=M+1}^{\infty} k_n \bar{a}_n \psi_n(x) + \sum_{n=0}^{M} k_n (\bar{a}_n - \hat{a}_n)\psi_n(x)\right)^2 \rho(x)\mathrm{d}x. \end{aligned} \tag{29}$$

The right hand side of Eq. (29) can be expanded to yield

$$\begin{aligned}\|\hat{E}_M\|^2 &= \int_\Gamma \left(\sum_{n=M+1}^{\infty}\sum_{m=M+1}^{\infty} k_n k_m \bar{a}_n \bar{a}_m \psi_n(x)\psi_m(x)\right)\rho(x)\mathrm{d}x \\ &\quad + \int_\Gamma \left(\sum_{n=0}^{M}\sum_{m=0}^{M} k_n k_m (\bar{a}_n - \hat{a}_n)(\bar{a}_m - \hat{a}_m)\psi_n(x)\psi_m(x)\right)\rho(x)\mathrm{d}x \\ &\quad + \int_\Gamma 2\left(\sum_{n=M+1}^{\infty}\sum_{m=0}^{M} k_n k_m \bar{a}_n (\bar{a}_m - \hat{a}_m)\psi_n(x)\psi_m(x)\right)\rho(x)\mathrm{d}x. \end{aligned} \tag{30}$$

Using the orthogonality property of the basis functions, the integrals in Eq. (30) can be reduced to

$$\|\hat{E}_M\| = \sqrt{\left(\sum_{n=M+1}^{\infty} \bar{a}_n^2 k_n\right) + \left(\sum_{n=0}^{M} (\bar{a}_n - \hat{a}_n)^2 k_n\right)}. \tag{31}$$

The first term under the radical in Eq. (31) is the truncation error due to approximating a continuous function with a finite series expansion. The second term gives the contribution to the total error due to statistical uncertainty in the expansion coefficients.

Eq. (31) demonstrates that the FET contains sources of both statistical error and truncation error. The presence of statistical uncertainty in Eq. (31) means that $\|\hat{E}_M\|$ is itself a random variable. Therefore, in order to analyze the convergence behavior of the FET we should consider the root-mean-square (RMS) error for simulations using N independent histories. The RMS error can be calculated directly from Eq. (31),

$$\sqrt{\left\langle \|\hat{E}_M\|^2 \right\rangle} = \sqrt{\left(\sum_{n=M+1}^{\infty} \bar{a}_n^2 k_n\right) + \left\langle \sum_{n=0}^{M} (\bar{a}_n - \hat{a}_n)^2 k_n \right\rangle}, \tag{32}$$

where angle brackets $\langle\rangle$ have been used to denote the expected value of a statistical quantity.

First, we will evaluate the statistical uncertainty term. Algebraically expanding and applying the expectation operator to each term in the summation yields,

$$\left\langle \sum_{n=0}^{M} (\bar{a}_n - \hat{a}_n)^2 k_n \right\rangle = \left(\sum_{n=0}^{M} \langle \hat{a}_n^2 \rangle k_n - \bar{a}_n^2 k_n\right). \tag{33}$$

By the definition of the variance of $\hat{a}_n$,

$$\langle \hat{a}_n^2 \rangle = \sigma_{\hat{a}_n}^2 + \bar{a}_n^2. \tag{34}$$

Substituting Eq. (34) into Eq. (33) shows that the statistical error in the functional approximation is related to the sum of the variances of the individual expansion coefficients,

$$\left\langle \sum_{n=0}^{M} (\bar{a}_n - \hat{a}_n)^2 k_n \right\rangle = \sum_{n=0}^{M} k_n \sigma_{\hat{a}_n}^2. \tag{35}$$

Using Eqs. (14) and (35) the statistical uncertainty term can be written as

$$\left\langle \sum_{n=0}^{M} (\bar{a}_n - \hat{a}_n)^2 k_n \right\rangle = \sum_{n=0}^{M} \frac{k_n}{N} \left(\int_\Gamma (\psi_n(x)\rho(x))^2 P(x) \mathrm{d}x - \bar{a}_n^2 \right), \tag{36}$$

and so

$$\left\langle \sum_{n=0}^{M} (\bar{a}_n - \hat{a}_n)^2 k_n \right\rangle \leqslant \sum_{n=0}^{M} \frac{k_n}{N} \left(\operatorname*{Max}_\Gamma (|\rho(x)P(x)|) \int_\Gamma \psi_n^2(x)\rho(x)\mathrm{d}x - \bar{a}_n^2 \right). \tag{37}$$

It should be noted that Eq. (37) is only valid if the function $|\rho(x)P(x)|$ is finite over the domain Γ. In cases where $|\rho(x)P(x)|$ is unbounded, special care may need to be taken to ensure that the technique will behave as expected.

Using the definition of k_n from Eq. (11) in Eq. (37) yields

$$\left\langle \sum_{n=0}^{M} (\bar{a}_n - \hat{a}_n)^2 k_n \right\rangle \leqslant \frac{1}{N} \sum_{n=0}^{M} \left[\operatorname*{Max}_\Gamma (|\rho(x)P(x)|) - \bar{a}_n^2 k_n \right],$$

and so

$$\left\langle \sum_{n=0}^{M} (\bar{a}_n - \hat{a}_n)^2 k_n \right\rangle \leqslant \frac{M}{N} \operatorname*{Max}_\Gamma (|\rho(x)P(x)|) - \frac{1}{N} \sum_{n=0}^{M} \bar{a}_n^2 k_n. \tag{38}$$

Further inspection of Eq. (38) reveals that the second term on the right hand side is always negative and can therefore be omitted without affecting the inequality. With this simplification Eq. (38) can be written

$$\left\langle \sum_{n=0}^{M} (\bar{a}_n - \hat{a}_n)^2 k_n \right\rangle \leqslant \frac{M}{N} \operatorname*{Max}_\Gamma (|\rho(x)P(x)|) \qquad \text{(expected statistical error)}. \tag{39}$$

Next, we evaluate the truncation error term from Eq. (31) using the convergence rate of the expansion coefficients given in Eq. (27),

$$\sum_{n=M+1}^{\infty} \bar{a}_n^2 k_n = \sum_{n=M+1}^{\infty} O\left[\frac{1}{n^{2\kappa}}\right] k_n \qquad \text{(truncation error)}. \tag{40}$$

Finally, the results from Eqs. (39) and (40) can then be used to rewrite Eq. (31) as

$$\sqrt{\left\langle \|\hat{E}_M\|^2 \right\rangle} \leqslant \sqrt{\frac{M}{N} \operatorname*{Max}_\Gamma (|\rho(x)P(x)|) + \sum_{n=M+1}^{\infty} \mathrm{O}\left[\frac{1}{n^{2\kappa}}\right] k_n}. \tag{41}$$

The detailed convergence behavior of Eq. (41) depends on both κ for the function $P(x)$ and the behavior of the series $\{k_n\}$.

The expression for the total (statistical + truncation) error can be written, to leading orders, as,

$$\sqrt{\left\langle \|\hat{E}_M\|^2 \right\rangle} \leqslant \sqrt{\mathrm{O}\left[\frac{M}{N}\right] + \sum_{n=M+1}^{\infty} \mathrm{O}\left[\frac{1}{n^{2\kappa}}\right] k_n}. \tag{42}$$

Eq. (42) demonstrates that the rate of convergence is determined not only by the smoothness of the function $P(x)$, but also by the ratio of the expansion order M to the number of histories run N. This divergent term

indicates that, for a fixed number of histories N, the total error in the approximation will begin to grow as more expansion orders are added.

4.3. Optimizing the FET approximation

Eq. (42) illustrates that the truncation error and statistical error terms in the FET are inversely related. The low order expansion coefficients are the easiest to integrate stochastically and will have smaller statistical uncertainties. However, using too few expansion coefficients will result in a large truncation error and low resolution. Using a higher order series expansion will decrease the truncation error, but higher expansion coefficients will always have larger statistical uncertainties because the basis functions are more difficult to integrate. Keeping too many, or poorly converged, coefficients will result in statistical error "contamination" of the final approximation. In order to obtain the maximum effectiveness from the FET, an optimal balance must be found between these two terms that will minimize the total error in the approximation.

Examination of Eqs. (32) and (35) shows, for each additional coefficient $\hat{a}_n$ included in the series, the truncation error is reduced by $\hat{a}_n^2$ and the statistical error is increased by $\hat{\sigma}^2_{\hat{a}_n} k_n$. Taking the ratio of the increase in statistical error to the decrease in truncation error,

$$R_n^2 = \frac{\hat{\sigma}^2_{\hat{a}_n} k_n}{\hat{a}_n^2}, \tag{43}$$

gives a relative cost-to-benefit metric associated with adding the nth term to the series. Note that $\sqrt{R_n^2}$ looks similar to the relative standard deviation that is widely used for standard Monte Carlo tallies; the two metrics differ only by a factor of $\sqrt{k_n}$.

This cost-to-benefit ratio provides a convenient test for determining how many expansion coefficients should be used from a given Monte Carlo simulation. Terms with values of $R_n^2 \gg 1$ should not be included in a functional approximation because they are not well converged and will not add any useful information to the result. Terms with values of $R_n^2 \ll 1$, on the other hand, should be included in the series approximation because they provide valuable information about the shape of the true function. Terms with $R_n^2 \approx 1$ are near the break even point and should be carefully examined before including any such term in a functional approximation. Some numerical results demonstrating the behavior of the cost-to-benefit ratio will be presented in the next section.

5. Numerical verification of FET convergence

We now present a series of numerical experiments designed to verify the theoretical convergence rate of the FET given in Eq. (42). In these experiments Monte Carlo simulations were used to estimate Legendre functional approximations to an arbitrarily chosen distribution for $P(x)$. The 2-norm of the residual error between the functional approximation and the exact distribution of $P(x)$ was then calculated for different expansion orders and numbers of histories.

The same trial distribution for $P(x)$ was used in each numerical experiment,

$$P(x) = \frac{1}{1.51985} \begin{cases} \cos(x)\mathrm{e}^{2x+1}, & x \in [-1, -1/2], \\ \cos(x), & x \in [-1/2, 1/2], \\ \cos(x)\mathrm{e}^{-x/2+1/4}, & x \in [1/2, 1]. \end{cases} \tag{44}$$

The distribution in Eq. (44) was chosen to reproduce many of the minimum requirements of distributions encountered during many Monte Carlo simulations. The distribution is continuous over the domain $(-1, 1)$ and piecewise smooth with discontinuities in the first derivative of the distribution occurring at $x = \pm 1/2$.

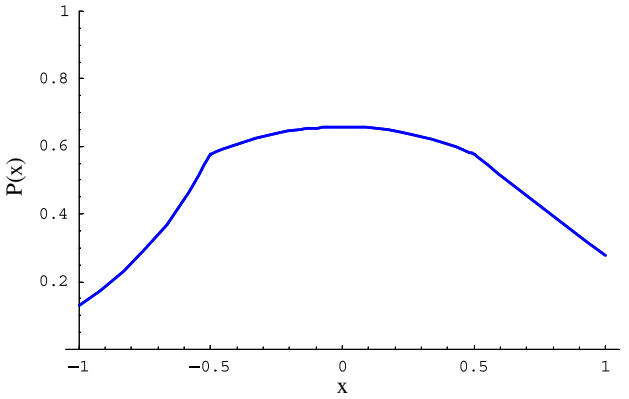

Fig. 1. Plot of reference distribution of $P(x)$ used for numerical verification of theoretical convergence results for the FET.

Because $P(x)$ is piecewise smooth it has two integrable derivatives and, therefore, an algebraic index of convergence $\kappa = 2$. A plot of the reference distribution is shown in Fig. 1.

5.1. Analytical FET approximation results

For testing purposes, functional approximations of $P(x)$ in the set of Legendre polynomials were considered. The Legendre polynomials are a complete set of basis functions that are orthogonal over the range $[-1, 1]$ with respect to the weighting function $\rho(x) = 1$. The normalization constants for the Legendre polynomials are

$$k_n = \frac{2n+1}{2}. \tag{45}$$

For comparative purposes the exact Legendre expansion coefficients for $P(x)$ were calculated using Eq. (10). A plot of the absolute values of the first 50 exact expansion coefficients is shown in Fig. 2. In the derivation of the convergence properties of the FET it was established in Eq. (27) that the expansion coeffi-

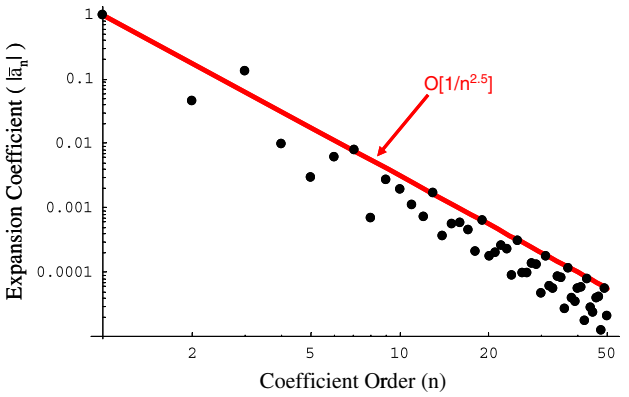

Fig. 2. Exact Legendre expansion coefficients for $P(x)$ plotted against Legendre expansion order. A $1/n^{2.5}$ trend line is shown for comparative purposes, indicating the convergence rate of the expansion coefficients.

cients should converge algebraically with an asymptotic bound of $O[n^{-\kappa}]$. Numerical results, shown in Fig. 2, give the index of convergence for $P(x)$ as $\kappa \approx 2.5$, slightly faster than the $\kappa = 2$ bound for a piecewise smooth function.

It was also established that the truncation error for a finite Legendre series approximation will converge as the expansion coefficients tend to zero. By using the result given in Eq. (40), the truncation error can be written concisely as

$$\|E_M\| = \sqrt{\sum_{n=M+1}^{\infty} \bar{a}_n^2 k_n} = \sqrt{\sum_{n=M+1}^{\infty} O\left[\frac{1}{n^{2\kappa}}\right] k_n}. \tag{46}$$

For the reference distribution of $P(x)$ in the set of Legendre polynomials, Eq. (46) predicts that the truncation error should converge at least as fast as

$$\|E_M\| = \sqrt{\sum_{n=M+1}^{\infty} O\left[\frac{1}{n^5}\right] \frac{2n+1}{2}} \leqslant O\left[\frac{1}{\sqrt{M^3}}\right]. \tag{47}$$

To demonstrate this convergence behavior, the exact Legendre expansion coefficients were used to construct functional approximations to $P(x)$ for values of M ranging from 0 to 49. For each order of exact functional approximation, the 2-norm truncation error was calculated directly by

$$\|E_M\| = \sqrt{\int_{-1}^{1} (P(x) - P_M(x))^2 \mathrm{d}x}. \tag{48}$$

The results, Fig. 3, show that the truncation error converges at the rate $O[1/\sqrt{M^3}]$, as expected. These results verify that a Legendre expansion of the reference distribution has the convergence properties predicted by the classical results for such expansions and provides a measured value for the algebraic index of convergence κ.

5.2. Stochastic FET approximation results

Additional studies were conducted to examine the convergence properties of a Legendre approximation to $P(x)$ that uses stochastically estimated expansion coefficients. For these studies, random samples were

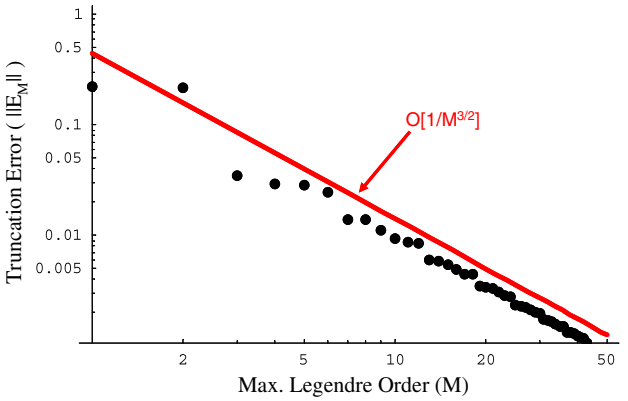

Fig. 3. Two norm measure of truncation error for a Legendre expansion approximation of $P(x)$ plotted against Legendre truncation order. A $1/M^{3/2}$ trend line is shown for comparative purposes, indicating the approximate convergence rate.

taken (via rejection sampling) from the distribution $P(x)$, given in Eq. (44). These samples were then used in Eq. (12) to estimate the Legendre expansion coefficients for $P(x)$.

In the previous section it was shown, Eq. (34), that the expected statistical error in a Monte Carlo estimate of an expansion coefficient is proportional to the true variance of $\hat{a}_n$, or

$$\langle|\hat{a}_n - \bar{a}_n|\rangle = \sqrt{\frac{1}{N}\left(\int_\Gamma (\psi_n(x)\rho(x))^2 P(x)\mathrm{d}x - \bar{a}_n^2\right)}. \tag{49}$$

Eq. (49) can be further simplified by using Eq. (37), to yield

$$\langle|\hat{a}_n - \bar{a}_n|\rangle \leqslant \sqrt{\frac{1}{N}\left(\frac{\underset{\Gamma}{\mathrm{Max}}\,(|\rho(x)P(x)|)}{k_n} - \bar{a}_n^2\right)}. \tag{50}$$

For the trial distribution of $P(x)$ and the basis set of Legendre polynomials, Eq. (50) can be evaluated directly,

$$\langle|\hat{a}_n - \bar{a}_n|\rangle \leqslant \sqrt{\frac{1}{N}\left(\frac{1.3159}{2n+1} - \bar{a}_n^2\right)}. \tag{51}$$

For a fixed sample size N and large values of n, Eq. (51) behaves, to leading order, as

$$\langle|\hat{a}_n - \bar{a}_n|\rangle \leqslant \mathrm{O}\left[\sqrt{\frac{1}{2n+1}}\right]. \tag{52}$$

It was previously established in Eq. (27) that the true expansion coefficients $|\bar{a}_n|$ will converge with order $\mathrm{O}[1/n^{2.5}]$. Thus, for large n, the true expansion coefficients $\bar{a}_n$ will be very close to zero, and statistical error will dominate the convergence rate of the stochastically estimated expansion coefficients. Substituting the approximation $\bar{a}_n = 0$ (for large n) into Eq. (52) gives

$$\langle|\hat{a}_n|\rangle \leqslant \mathrm{O}\left[\sqrt{\frac{1}{2n+1}}\right] \tag{53}$$

as the convergence rate for stochastically estimated coefficients. To test this convergence rate the first 1000 expansion coefficients for $P(x)$ were estimated in a 10,000 history Monte Carlo simulation. The results, given in Fig. 4, show that the absolute value of the statistical error in the expansion coefficients converges as $\mathrm{O}[1/\sqrt{2n+1}]$. This agrees with the predicted behavior given in Eq. (52).

Theoretical results predict that the total error in a stochastic FET approximation to $P(x)$ will behave as the sum of two independent terms: the truncation error, which will converge as the expansion order increases; and the statistical error, which is divergent with increasing expansion order for a constant sample size. The general form for the 2-norm measure of residual error was given in Eq. (42). For the trial distribution of $P(x)$ the expected convergence rate can be evaluated using Eqs. (42) and (47),

$$\sqrt{\left\langle \|\hat{E}_M\|^2 \right\rangle} = \sqrt{\mathrm{O}\left[\frac{M}{N}\right] + \mathrm{O}\left[\frac{1}{\sqrt{M^3}}\right]}. \tag{54}$$

To verify this convergence behavior, a 10,000 history Monte Carlo simulation was used to estimate the first 1000 Legendre expansion coefficients. These expansion coefficients were used to construct functional approximations with orders from 0 to 1000. For each order of functional approximation, the exact 2-norm error was calculated directly from Eq. (48).

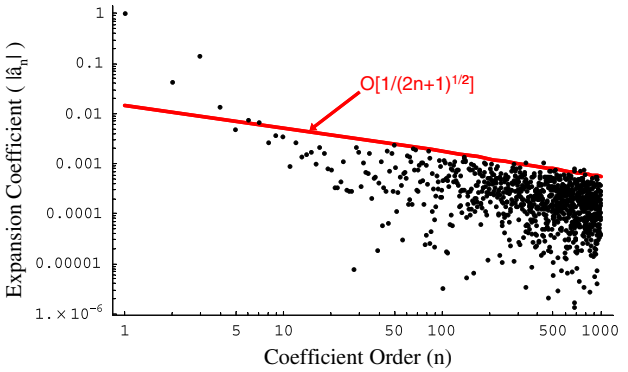

Fig. 4. Monte Carlo estimated Legendre expansion coefficients for $P(x)$ plotted against Legendre expansion order. Each expansion coefficient was estimated using the same 10,000 history random walk process. A $1/(2n+1)^{1/2}$ trend line is shown for comparative purposes, indicating the theoretical convergence rate.

The results, given in Fig. 5, show that there is an optimal expansion order that minimizes the residual error of the approximation. This optimal order, which is around 9 for this test problem, is the point where the statistical uncertainty in the expansion coefficients begins to contaminate the approximation. Below this optimal order, each added expansion term improves the functional approximation by reducing the truncation error of the series expansion. Above the optimal expansion order, the residual error begins to diverge at the O[M/N] rate predicted by Eq. (54) (or the equivalent Eq. (42)). The optimal expansion order also depends on the number of histories used in the Monte Carlo simulation. As more histories are used, the uncertainty associated with all of the coefficients is reduced, allowing more terms to be included in an expansion without contaminating the overall solution. Thus, as the number of histories in the simulation is increased the optimal value will begin to shift towards larger values, and the minimum total error will decrease. This behavior is illustrated in Fig. 6.

5.3. Estimating the optimal expansion order

The results shown in Fig. 6 demonstrate that for every simulation there exists an optimal order FET expansion that gives the highest accuracy (in the 2-norm) approximation. In the benchmark problem

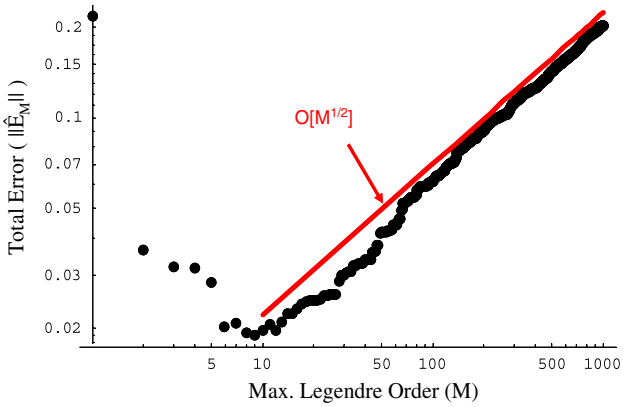

Fig. 5. Two norm measure of total error for a stochastic Legendre expansion approximation to plotted $P(x)$ against Legendre truncation order. Each expansion coefficient was estimated using the same $N = 10{,}000$ history random walk process.

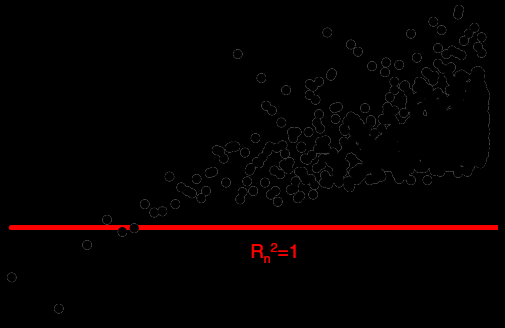
$R_n^2=1$

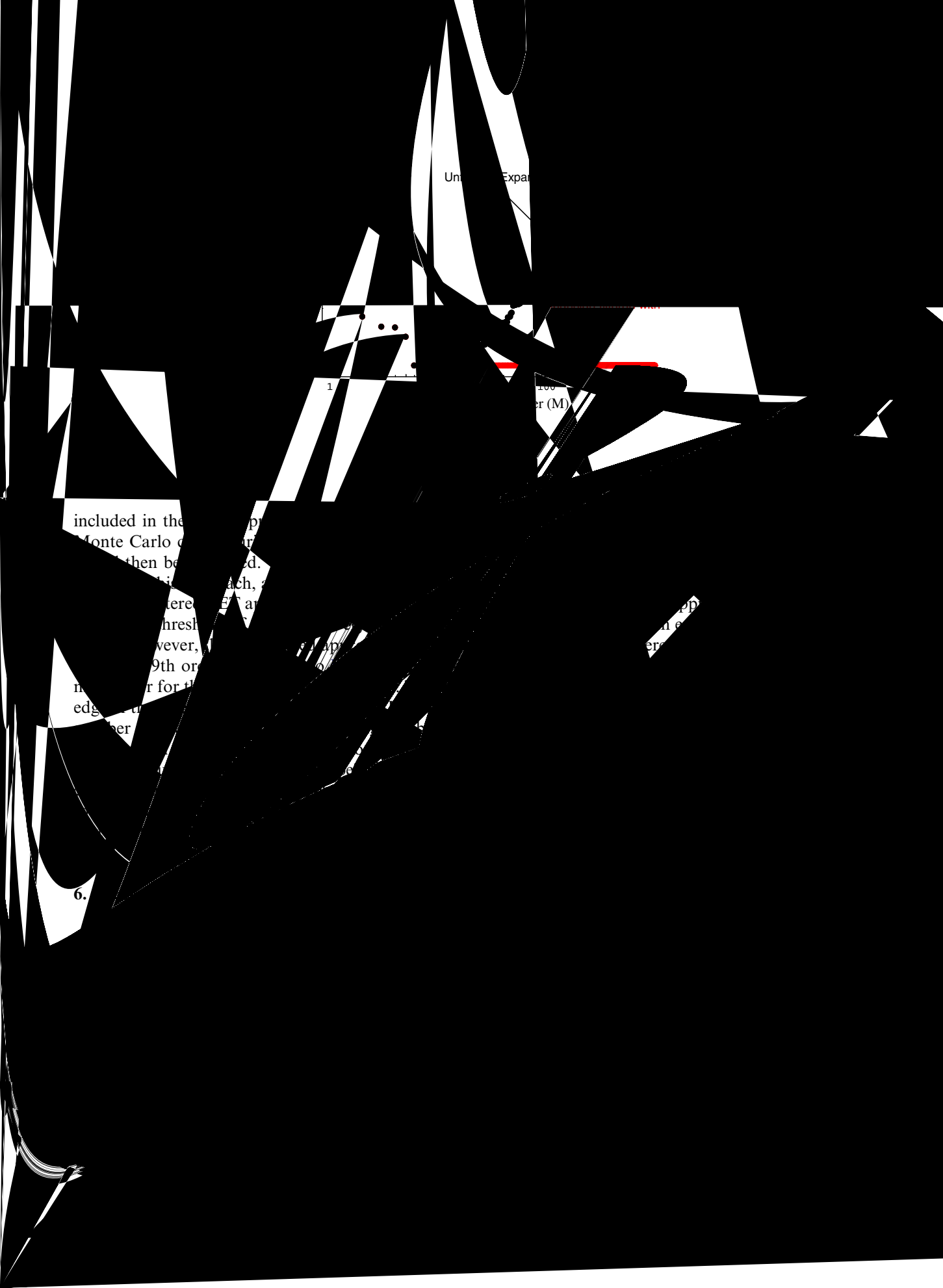

included in the
Monte Carlo
then be
ed.
ach,
ere
hresh
vever,
9th or
r for t
edg
ber

6.

In Eq. (55) the set $\{x_0, x_1, \ldots, x_{M-1}, x_M\}$ represents the bin boundaries for an M bin histogram, assuming 1-D for convenience. In order to simplify the following analysis, we assume that each bin of the histogram is of equal width Δx. The 2-norm measure of the residual error between the true function and the best-fit histogram approximation can be written

$$\|E_M^{\text{hist}}\| = \|P(x) - \overline{P_M^{\text{hist}}}(x)\| = \sqrt{\int_{x_0}^{x_M} \left(P(x) - \overline{P_M^{\text{hist}}}(x)\right)^2 \rho(x)\mathrm{d}x}. \tag{56}$$

Because the histogram approximation is constant over each bin, it is convenient to write the integral on the right hand side of Eq. (56) as

$$\|E_M^{\text{hist}}\| = \sqrt{\sum_{b=1}^{M} \int_{x_{b-1}}^{x_b} \left(P(x) - \overline{P_{M,b}^{\text{hist}}}\right)^2 \mathrm{d}x}, \tag{57}$$

where $\overline{P_{M,b}^{\text{hist}}}$ is the value of the bth histogram bin. By Taylor expanding $P(x)$ about the midpoint of each bin and simplifying, Eq. (57) yields, to leading order,

$$\|E_M^{\text{hist}}\| = \sqrt{\sum_{b=1}^{M} \mathrm{O}[\Delta x^3]}. \tag{58}$$

Eq. (58) gives the truncation error of the approximation as a function of the bin width instead of the total number of bins. For a bounded interval of length L divided into M equal bins, Δx is inversely proportional to the number of bins,

$$\Delta x = \frac{L}{M}. \tag{59}$$

With this assumption, Eq. (58) can be rewritten in terms of the number of histogram bins used,

$$\|E_M^{\text{hist}}\| = \sqrt{\sum_{b=1}^{M} \mathrm{O}\left[\frac{1}{M^3}\right]}. \tag{60}$$

Since there are M bins, each with error $\mathrm{O}[1/M^3]$ it follows immediately that the total truncation error is

$$\|E_M^{\text{hist}}\| = \sqrt{\mathrm{O}\left[\frac{1}{M^2}\right]} = \mathrm{O}\left[\frac{1}{M}\right] \qquad \text{(truncation error)}. \tag{61}$$

A comparison of the FET and histogram truncation error convergence rates, Eqs. (40) and (61), demonstrates that the FET will asymptotically converge to the correct distribution faster than a histogram approximation in cases where

$$\sqrt{\sum_{n=M+1}^{\infty} \mathrm{O}\left[\frac{k_n}{n^{2\kappa}}\right]} < \mathrm{O}\left[\frac{1}{M}\right]. \tag{62}$$

Evaluating the infinite series in the first term for $M \gg 1$ shows that Eq. (62) will hold as long as

$$\frac{k_n}{n^{2\kappa}} < \mathrm{o}\left[\frac{1}{n^3}\right]. \tag{63}$$

The terms k_n and κ in Eqs. (62) and (63) illustrate that the convergence properties of the FET depend on both the smoothness of the function $P(x)$, as well as the set of basis functions chosen for the expansion. For

the case of a Legendre polynomial expansion of a probability distribution with $\kappa = 2.5$, such as the example shown in Section 5, Eq. (63) gives

$$\frac{k_n}{n^{2\kappa}} = \frac{2n+1}{2n^5} = \frac{1}{n^4} + \frac{1}{2n^5} < \mathrm{o}\left[\frac{1}{n^3}\right]. \tag{64}$$

Eq. (64) indicates that the FET approximation will converge to the true distribution faster than a histogram approximation. This implies that a functional expansion tally of order M may provide a more accurate estimate of the true distribution than a histogram approximation with M bins.

It is important to note that Eq. (63) applies only to the asymptotic truncation error convergence rates for the FET and histogram approximations. Convergence properties at low approximation orders do not necessarily follow these asymptotic limits. As such, Eq. (63) should only be used as a rough guide for selecting a tally method. Furthermore, Eq. (63) should only be used when a minimal amount of a priori information, such as continuity or smoothness, is available for the unknown distribution. If more detailed information about the distribution is known, then it may be possible to tailor an optimal tally, by either selecting a more suitable set of orthogonal basis functions, in the case of the FET, or choosing a non-uniform set of bin widths in the histogram method. Obviously the best possible scenario is to choose a basis set that fits the unknown distribution exactly with the minimum number of terms.

6.2. Statistical error

When a histogram is created from a Monte Carlo calculation, each estimated bin height has some degree of statistical uncertainty. The variance of each bin estimate is directly related to the number of histories that score in that particular bin. This uncertainty can be accounted for in the analysis by including a random noise term ε in each bin of the histogram definition, Eq. (55),

$$\widehat{P^{\mathrm{hist}}_{M,b}} = \frac{1}{\Delta x}\int_{x_{b-1}}^{x_b} P(x)\mathrm{d}x + \varepsilon_b \qquad \forall x \in [x_{b-1}, x_b]. \tag{65}$$

The ε term is a zero-mean random variable [26] that describes the distribution of statistical error in the estimate of $P^{\mathrm{hist}}_M(x)$. Although the notation is slightly different, this analysis of statistical error is identical to that used for the FET. A Taylor expansion of $P(x)$ about the midpoint $x_{b-1/2}$ of a bin in Eq. (65) yields

$$\left(P(x) - \widehat{P^{\mathrm{hist}}_{M,b}}\right) = \varepsilon_b - \frac{P''(x_{b-1/2})}{6}\Delta x^2 + \mathrm{O}[\Delta x^4]. \tag{66}$$

The total error for the histogram approximation, including statistical uncertainty, can be written

$$\|\hat{E}^{\mathrm{hist}}_M\| = \sqrt{\sum_{b=1}^{M}\int_{x_{b-1}}^{x_b}\left(P(x) - \widehat{P^{\mathrm{hist}}_{M,b}}\right)^2 \mathrm{d}x}. \tag{67}$$

Substituting Eq. (66) into Eq. (67) gives,

$$\|\hat{E}^{\mathrm{hist}}_M\| = \sqrt{\sum_{b=1}^{M}\int_{x_{b-1}}^{x_b}\left(\varepsilon_b - \frac{P''(x_{b-1/2})}{6}\Delta x^2 - \mathrm{O}[\Delta x^4] + P'(x_{b-1/2})x + \frac{P''(x_{b-1/2})}{2}x^2 + \mathrm{O}[x^3]\right)^2 \mathrm{d}x}. \tag{68}$$

Expanding Eq. (68) and integrating,

$$\|\hat{E}^{\mathrm{hist}}_M\| = \sqrt{\sum_{b=1}^{M}\varepsilon_b^2\Delta x + \frac{P'(x_{b-1/2})^2\Delta x^3}{3} + \mathrm{O}[\Delta x^5]}. \tag{69}$$

Eq. (69) gives the 2-norm of the residual error in terms of ε_b, the statistical uncertainty in the estimate of $\widehat{P^{\text{hist}}_{M,b}}$. According to the Central Limit Theorem, this random variable will be normally distributed with mean zero and variance $\sigma^2_{\widehat{P^{\text{hist}}_{M,b}}}$. As with the FET analysis, the presence of statistical uncertainty in Eq. (69) means that $\|\hat{E}^{\text{hist}}_M\|$ is a random variable. To proceed, we consider the RMS expected value of $\|\hat{E}^{\text{hist}}_M\|$,

$$\sqrt{\left\langle \|\hat{E}^{\text{hist}}_M\|^2 \right\rangle} = \sqrt{\sum_{b=1}^{M} \langle \varepsilon_b^2 \rangle \Delta x + \frac{P'(x_{b+1/2})^2 \Delta x^3}{3} + \mathrm{O}[\Delta x^5]}. \tag{70}$$

Using the definition of $\sigma^2_{\widehat{P^{\text{hist}}_{M,b}}}$ for a random variable with a mean of zero, it is possible to express the expected value of the statistical error squared as

$$\left\langle \varepsilon_b^2 \right\rangle = \sigma^2_{\widehat{P^{\text{hist}}_{M,b}}}. \tag{71}$$

Using Eq. (71) in Eq. (70) yields an intermediate form for the expected 2-norm error of the histogram approximation, which contains the bin variance $\sigma^2_{\widehat{P^{\text{hist}}_{M,b}}}$ instead of a random noise term ε_b,

$$\sqrt{\left\langle \|\hat{E}^{\text{hist}}_M\|^2 \right\rangle} = \sqrt{\sum_{b=1}^{M} \sigma^2_{\widehat{P^{\text{hist}}_{M,b}}} \Delta x + \frac{P'(x_{b-1/2})^2 \Delta x^3}{3} + \mathrm{O}[\Delta x^5]}. \tag{72}$$

The bin variance can be derived by recognizing that the estimator for $\widehat{P^{\text{hist}}_{M,b}}$ is simply the number of histories that score in bin b, denoted N_b. For such a case it is easy to show that the relative uncertainty in each bin obeys traditional counting statistics,

$$\frac{\sigma_{\widehat{P^{\text{hist}}_{M,b}}}}{\widehat{P^{\text{hist}}_{M,b}}} = \frac{1}{\sqrt{N_b}}. \tag{73}$$

The expected number of counts in each bin is equal to the ratio of the integral over the bin to the integral over all bins,

$$\langle N_b \rangle = \frac{\int_{x_{b-1}}^{x_b} P(x)\mathrm{d}x}{\int_{x_0}^{x_M} P(x)\mathrm{d}x} N. \tag{74}$$

Using Eqs. (73) and (74) to solve for $\left\langle \sigma_{\widehat{P^{\text{hist}}_{M,b}}} \right\rangle$ yields,

$$\left\langle \sigma_{\widehat{P^{\text{hist}}_{M,b}}} \right\rangle = \frac{\overline{P^{\text{hist}}_{M,b}} \sqrt{\int_{x_0}^{x_M} P(x)\mathrm{d}x}}{\sqrt{N \int_{x_{b-1}}^{x_b} P(x)\mathrm{d}x}} = \frac{\overline{P^{\text{hist}}_{M,b}}}{\sqrt{N \int_{x_{b-1}}^{x_b} P(x)\mathrm{d}x}}, \tag{75}$$

which simplifies by using Eq. (55),

$$\left\langle \sigma_{\widehat{P^{\text{hist}}_{M,b}}} \right\rangle = \frac{\sqrt{\overline{P^{\text{hist}}_{M,b}}}}{\sqrt{\Delta x N}}. \tag{76}$$

Finally, Eq. (59) can be used to write the standard deviation in terms of the total number of histogram bins,

$$\left\langle \sigma_{\widehat{P^{\text{hist}}_{M,b}}} \right\rangle = \sqrt{\frac{M\overline{P^{\text{hist}}_{M,b}}}{N}}. \tag{77}$$

Eqs. (77) and (55) can be used to simplify Eq. (72),

$$\sqrt{\left\langle \|\hat{E}^{\text{hist}}_M\|^2 \right\rangle} = \sqrt{\frac{M}{N}\sum_{b=1}^{M}\int_{x_{b-1}}^{x_b} P(x)\mathrm{d}x + \sum_{b=1}^{M}\frac{P'(x_{b-1/2})^2}{3M^3} + \mathrm{O}\left[\frac{1}{M^5}\right]}. \tag{78}$$

The summation over all bins in the first term under the radical produces an integral over the entire distribution and evaluates to 1,

$$\sqrt{\left\langle \|\hat{E}^{\text{hist}}_M\|^2 \right\rangle} = \sqrt{\frac{M}{N} + \sum_{b=1}^{M}\frac{P'(x_{b-1/2})^2}{3M^3} + \mathrm{O}\left[\frac{1}{M^5}\right]}. \tag{79}$$

Eq. (79) can then be written to leading order as

$$\sqrt{\left\langle \|\hat{E}^{\text{hist}}_M\|^2 \right\rangle} = \sqrt{\mathrm{O}\left[\frac{M}{N}\right] + \mathrm{O}\left[\frac{1}{M^2}\right]}. \tag{80}$$

Comparing Eqs. (80) and (42) shows that statistical uncertainty has the same effect on both the FET and the histogram tally, causing the 2-norm of the total error to diverge as order $\sqrt{M/N}$ for large values of M. This important result indicates that both methods behave qualitatively in a similar way. For any number of histories N, there is an optimal value of M that allows the most information about the functional shape to be obtained. Using a value of M that is larger than the optimal value will only result in the functional approximation becoming contaminated by modes (or bins) that are not well converged.

The preceding derivations have all assumed that all of the bins in the histogram approximation have equal width. With this equal width assumption, the 2-norm convergence for truncation error in the histogram tally is $1/M$ for functions with a nonzero first derivative.

7. Numerical results for histogram convergence

Using the test distribution for $P(x)$ given in Eq. (44), verification studies of the theoretical histogram tally convergence rates were conducted. We examined the convergence rate of the 2-norm residual error for histogram approximations using exact bin heights and different numbers of bins. For each histogram bin, values were calculated with Eq. (55) and the residual errors were calculated with Eq. (57). The results of this study, shown in Fig. 9, demonstrate that for $M \geqslant 2$, the residual error in the histogram approximation converges as O[$1/M$], the exact rate predicted in Eq. (61).

We then included the effect of statistical uncertainty on the convergence rate of the histogram approximation. Instead of calculating bin values directly, random samples were taken from the test distribution of $P(x)$ and tallied in the appropriate histogram bin. Bin values were then estimated by dividing the number of samples scoring in each bin by the total number of samples times the bin width. The residual error between the Monte Carlo histogram approximation and true distribution was calculated directly with Eq. (57).

The results, shown in Fig. 10, demonstrate that the convergence behavior of the truncation error behaves qualitatively as predicted in Eq. (80). Like the FET, for fixed N, the histogram has an optimal number of bins that will minimize the total residual error of the approximation. The optimal number of bins is approximately 20 for the test distribution considered. For a histogram approximation using more than the optimal number of bins, the residual error begins to increase as more bins are used.

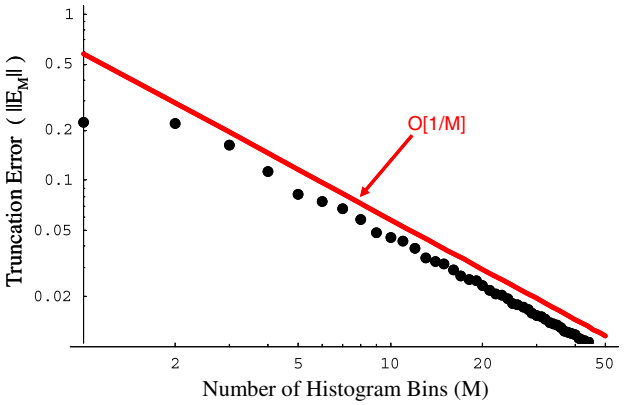

Fig. 9. Two norm measure of residual error for a histogram approximation to $P(x)$ plotted against the number of histogram bins. A $1/M$ trend line is shown for comparative purposes, indicating the convergence rate.

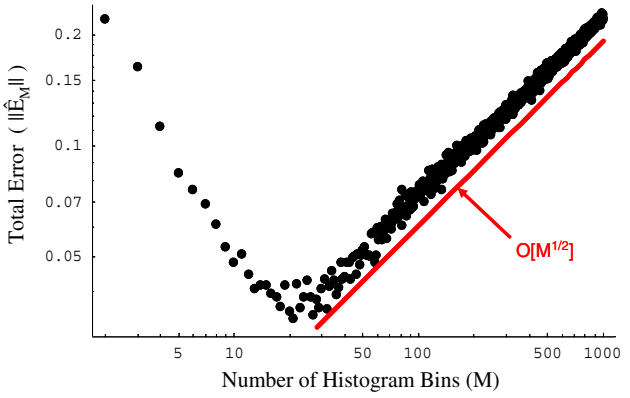

Fig. 10. Two norm measure of residual error for a stochastic histogram approximation to $P(x)$ plotted against the number of histogram bins used. Each histogram approximation was created using the same $N = 10{,}000$ samples from $P(x)$.

8. Discussion and comparison of results

We have already demonstrated, theoretically and numerically, that the FET and histogram approximations converge to the true distribution in qualitatively the same way as the approximation order is increased.

To compare the FET and histogram residual errors, Figs. 5 and 10 are shown plotted together in Fig. 11 This figure demonstrates that the FET and histogram approximations have roughly the same convergence behavior with respect to the approximation order M. Both methods show a reduction in residual error with increasing order before reaching an optimal value of M that minimized the total error. Below this optimal value the convergence is dominated by the truncation error inherent in each of the approximations. For approximation orders greater than the optimal value, the residual error begins to increase due to statistical noise in the system. In this case, the FET error is always less than the histogram error as $M \to \infty$.

Fig. 11 illustrates that, for the trial distribution of $P(x)$ selected, the FET is superior to the histogram tally. For a 10,000 history calculation, the FET can achieve a smaller residual error than a histogram approximation, for any order of approximation. Furthermore, the results show that a 4th or 5th order

Leg
FE

wi
m
tl
h

On the other hand, estimating higher moments within these histogra
improvement in the results, allowing piecewise FET to do very well in situ
priori knowledge regarding the location of discontinuities, such as at materi
port applications [17]. For homogeneous systems, or any case where smooth
pected, a Legendre of Chebyshev FET approximation will most likely sh
histogram tally.

9. Conclusions

We have examined the convergence properties of the FET to reconstru
samples obtained during a Monte Carlo simulation. Derivations for the g
their variances were presented. A detailed analysis was performed to deter
tional expansion converges to the true distribution as the expansion order i
demonstrate that this convergence behavior depends primarily on the smoo
but can also depend on the set of basis functions chosen for the expansion

The initial convergence rate of the FET for a non-analytic function was sh
determined by the algebraic index of convergence for the function. For analy
gence rate of the FET is exponential. Unfortunately, these convergence rates
uncertainty with order $O\left[\sqrt{M/N}\right]$, due to the stochastic nature of the Mon
For large values of the ratio M/N, the statistical uncertainty begins to domina
the highest order expansion coefficients. Due to these competing sources of
shows that, for a given number of histories run, there is an optimal expa
sum of the truncation error and statistical error in the final approximation

is a function of the number of particle histories used in the Monte Carlo calculation. The convergence of the FET with respect to the number of particle histories remains $O\left[1/\sqrt{N}\right]$ with fixed expansion order.

For comparative purposes, a similar convergence analysis was preformed for the traditional histogram tally. With increasing numbers of bins, the convergence behavior of the histogram approximation was shown to converge at a fixed rate of $O[M^{-1}]$, where M is the number of bins. As with the FET, statistical error in the histogram tally increases with order $O\left[\sqrt{M/N}\right]$, and consequently, there is an optimum number of histogram bins that minimizes the residual error of the approximation.

Numerical verification of the theoretical results was conducted with a sample distribution. The empirical results agreed with the theory and demonstrated, for the sample distribution chosen, that the FET provided a better approximation to the shape of the distribution than the histogram tally.

Although the FET and histogram tallies converge qualitatively in the same way, there are cases where one method can clearly outperform the other. For distributions that are at least piecewise smooth, the faster initial convergence rate of the FET can provide a better fit than a histogram approximation of the same order. However, for distributions that are only piecewise continuous (or contain very steep gradients) the histogram approximation may provide a better fit than the FET, especially if bin boundaries can be located at or near the functional discontinuities. However, in cases where the locations of discontinuities are known, a piecewise FET approximation can outperform both a histogram tally and a global FET approximation. The judicious choice of one of these methods based on any prior knowledge of the unknown distribution can ensure that the maximum amount of information is obtained from the Monte Carlo simulation.

Although the FET offers many benefits, it is not without limitations. End-users of the method must always bear in mind that the technique produces a truncated approximation to the true solution. Therefore, using an expansion with too few terms may produce an approximation that cannot resolve important features of the distribution. Furthermore, for the basis sets considered, there is no guarantee that a functional approximation will be positive everywhere, even though physics may require the true solution to be positive. In practice, such unphysical results have only been observed for distributions that one would not expect to be well represented by a series expansion in a set of continuous basis functions. Even in cases where the functional approximation becomes negative (or otherwise unphysical), the errors are localized and do not appear to significantly degrade the overall approximation [15,18].

Although the concepts of functional expansion tallies were published as early as 1975, each previous implementation of the method was uniquely tailored for a specific application. This paper seeks to illustrate that the FET is a powerful technique that may have far more applications than previously realized. The FET is a promising new tool that may allow end-users to extract more information from Monte Carlo simulations than has been previously available with conventional tallies.

Acknowledgements

The first author would like to acknowledge the educational support provided by the Naval Nuclear Propulsion Fellowship Program sponsored by Naval Reactors Division of the U.S. Department of Energy. The authors would also like to thank Prof. Ziya Akcasu for his helpful insights throughout our work.

References

[1] J.M. Hammersley, D.C. Handscomb, Monte Carlo Methods, John Wiley and Sons, New York, 1964.
[2] E.E. Lewis, W.F. Miller, Computational Methods of Neutron Transport, John Wiley and Sons, New York, 1984.
[3] J. Spanier, E.M. Gelbard, Monte Carlo Principles and Neutron Transport Problems, Addison-Wesley, Reading, 1969.

[4] S.A. Dupree, S.K. Fraley, A Monte Carlo Primer – A Practical Approach to Radiation Transport, Plenum, New York, 2002.
[5] A. Dubi, Monte Carlo Calculations for Nuclear Reactors, in: Y. Ronen (Ed.), CRC Handbook of Nuclear Reactors Calculations, CRC Press, Boca Raton, FL, 1986, pp. 1–86.
[6] L.L. Carter, E.D. Cashwell, Particle-Transport Simulation with the Monte Carlo Method, vol. TID-26608, Technical Information Center, Energy Research and Development Administration, Oak Ridge, 1975.
[7] E.D. Cashwell, C.J. Everett, A Practical Manual on the Monte Carlo Method for Random Walk Problems, vol. 1, Pergamon Press, New York, 1959.
[8] W.L. Chadsey, C.W. Wilson, V.W. Pine, X-ray photoemission calculations, IEEE Trans. Nucl. Sci. 22 (6) (1975) 2345–2350.
[9] B.L. Beers, V.W. Pine, Functional expansion technique for monte carlo electron transport calculations, IEEE Trans. Nucl. Sci. 23 (6) (1976) 1850–1856.
[10] A. Noel, H.S. Wio, A new series-expansion approach in Monte Carlo: application to neutron shielding, Ann. Nucl. Energy 11 (5) (1984) 225–227.
[11] D. Legrady, E.J. Hoogenboom, Monte Carlo Midway Forward-Adjoint Coupling with Legendre Polynomials for Borehole Logging Applications, in: Physor 2004 – The Physics of Fuel Cycles and Advanced Nuclear Systems: Global Developments, American Nuclear Society, Chicago, IL, 2004, p. on CD-ROM.
[12] D. Legrady, E.J. Hoogenboom, Visualization of Space-Dependency of Responses of Monte Carlo Calculations Using Legendre Polynomials, in: Physor 2004 – The Physics of Fuel Cycles and Advanced Nuclear Systems: Global Developments, American Nuclear Society, Chicago, IL, 2004, p. on CD-ROM.
[13] B.T. Rearden, Perturbation theory eigenvalue sensitivity analysis with Monte Carlo techniques, Nucl. Sci. Eng. 146 (2004) 367–382.
[14] D.P. Griesheimer, W.R. Martin, Two Dimensional Functional Expansion Tallies for Monte Carlo Simulations, in: Physor 2004 – The Physics of Fuel Cycles and Advanced Nuclear Systems: Global Developments, American Nuclear Society, Chicago, IL, 2004, p. on CD-ROM.
[15] D.P. Griesheimer, W.R. Martin, J.P. Holloway. Estimation of flux distributions with Monte Carlo functional expansion tallies, in: Tenth International Conference on Radiation Shielding (ICRS-10), 2004, Madeira, Portugal.
[16] J. Spanier, Monte Carlo Methods for flux expansion solutions of transport problems, Nucl. Sci. Eng. 133 (1999) 73–79.
[17] D.P. Griesheimer, W.R. Martin, Estimating the global scalar flux distribution with orthogonal function expansion, Trans. Am. Nucl. Soc. 89 (2003) 462–464.
[18] D.P. Griesheimer, W.R. Martin, Monte-Carlo based angular flux response functions, Trans. Am. Nucl. Soc. 89 (2003).
[19] D.P. Griesheimer, W.R. Martin, Two dimensional functional expansion tallies for Monte Carlo simulations, PHYSOR 2004 – The Physics of Fuel Cycles and Advanced Nuclear Systems: Global Developments, (2004) on CD-ROM.
[20] F.B. Brown, D.P. Griesheimer, W.R. Martin, Continuously Varying Material Properties and Tallies for Monte Carlo Calculations, in: Physor 2004 – The Physics of Fuel Cycles and Advanced Nuclear Systems: Global Developments, American Nuclear Society, Chicago, IL, 2004, p. on CD-ROM.
[21] B.W. Silverman, Density Estimation for Statistics and Data Analysis, vol. 26, Chapman and Hall, New York, 1986.
[22] M.E. Tarter, M.D. LockModel-Free Curve Estimation, vol. 56, Chapman and Hall, New York, 1993.
[23] G.B. Folland, Fourier Analysis and Its Applications, Brooks/Cole, Detroit, 1992.
[24] J.P. Boyd, Chebyshev and Fourier Spectral Methods, Springer-Verlag, New York, 1989.
[25] T.W. Körner, Fourier Analysis, Cambridge University Press, New York, 1988.
[26] A. Papoulis, Probability, Random Variables, and Stochastic Processes, third ed., McGraw-Hill, New York, 1991.